

Classification of premature cardiac contractions based on RFECV and ensemble learning

Elsa Sari Hayunah Nurdiniyah, A'isyah Nur Aulia Yusuf, Norma Amalia, Widhiatmoko Herry Purnomo, Azizah Najda Hafizha

Department of Electrical Engineering, Faculty of Engineering, Universitas Jenderal Soedirman, Purbalingga, Indonesia

Article Info

Article history:

Received Oct 2, 2025

Revised Feb 5, 2026

Accepted Mar 29, 2026

Keywords:

Ensemble learning

Machine learning

Premature atrial contractions

Premature cardiac contractions

Premature ventricular contractions

recursive feature elimination with cross-validation

ABSTRACT

Premature cardiac contractions, including premature atrial contractions (PACs) and premature ventricular contractions (PVCs), are common arrhythmias that may increase the risk of cardiovascular complications when they occur frequently. Accurate classification of these events from electrocardiogram (ECG) signals remains challenging due to noise and signal variability. This study proposes a machine learning-based classification framework that combines recursive feature elimination with cross-validation for feature selection and an ensemble learning strategy to improve classification robustness. The approach was evaluated using the Massachusetts Institute of Technology – Beth Israel Hospital (MIT-BIH) Arrhythmia database and achieved high classification performance, with an accuracy of 95.34%, F1-score of 92.11%, and balanced precision and recall for PVC and PAC. In addition, SHapley Additive exPlanations (SHAP) were employed to identify the most influential features, enhancing model interpretability. The results demonstrate that the proposed framework provides a reliable and interpretable solution for distinguishing premature cardiac contractions, highlighting its potential application in clinical decision support systems.

This is an open access article under the [CC BY-SA](https://creativecommons.org/licenses/by-sa/4.0/) license.



Corresponding Author:

Elsa Sari Hayunah Nurdiniyah

Department of Electrical Engineering, Faculty of Engineering, Universitas Jenderal Soedirman

Raya Mayjen Sungkono Street No. KM 5, Dusun 2, Blater, Purbalingga, Jawa Tengah, Indonesia 53371

Email: elsa.nurdiniyah@unsoed.ac.id

1. INTRODUCTION

Premature contractions are abnormal heartbeats that originate outside the sinoatrial node. Generally, these impulses originate in the atria or ventricles. If the impulse originates in the atrial region, it is called a premature atrial contraction (PAC), and if the impulse originates in the ventricular region, it is called a premature ventricular contraction (PVC). PACs are generally considered benign and often require no treatment, occurring across all age groups with increasing prevalence in older populations [1]. However, excessive PACs have been associated with pathological changes in the left atrium and increased risks of atrial fibrillation, stroke, mortality, atrial cardiomyopathy, and kidney disorders, indicating broader systemic complications involvement even in patients without a prior history of atrial fibrillation [2]–[5]. Similarly, PVC is also considered a generally harmless cardiac abnormality [6]. In certain conditions, frequent PVCs are associated with an increased risk of atrial fibrillation and ischaemic stroke and may contribute to arrhythmias and cardiomyopathy [7]–[9]. Notably, PVCs are one of the most common forms of abnormal heartbeat and have serious consequences, especially in the elderly population [10].

Generally, heart rhythm abnormalities, such as premature contractions, are detected using an electrocardiogram (ECG). Unfortunately, manual interpretation of ECG signals requires high expertise, is time-

consuming, and is prone to errors due to noise and subjectivity. Recent advances in machine learning have enabled automated arrhythmia classification showing promising results. Various machine learning algorithms have been widely used in heartbeat classification, including K-nearest neighbors (KNN) [11]–[14], support vector machine (SVM) [15], [16], light gradient boosting machine (LightGBM) [17], [18]. The use of these algorithms shows fairly good performance, but an approach that combines several methods known as ensemble learning (EL) often provides more optimal performance [19]–[22]. This is due to the ability of EL to combine the strengths of each algorithm, resulting in a more comprehensive and robust classification model compared to using a single model.

Research on premature cardiac contraction classification remains limited, with most existing studies focusing primarily on PVC. Studies that address both PAC and PVC often exhibit significant performance imbalance between the two classes (PAC and PVC) [23]–[27]. Furthermore, many studies have not applied an inter-patient scenario, which involves testing the model on data from patients not used in the training stage [22], [28]; thus, the model's ability to generalize to new patients remains weak. In a clinical context, inter-patient generalisation is crucial due to physiological variations between individuals. This condition indicates that, despite numerous features being considered, there is no robust feature selection step to determine which features are truly informative in distinguishing between PAC, PVC, and normal classes, as well as to maintain performance when the model is applied to unseen data.

Therefore, this study uses recursive feature elimination with cross-validation (RFECV) as a feature selection method in the premature cardiac contraction classification model. RFECV eliminates the features gradually during cross-validation at each step, allowing for the identification of the most informative feature subset while assessing model performance between folds. Several studies have demonstrated the effectiveness of feature selection methods in disease classification, particularly through the application of RFECV. For example, in this research RFECV successfully selected 25 out of approximately 128 ECG-phonocardiogram (PCG) features, thereby improving model accuracy [29]. Another study also demonstrated that the use of RFECV on heart disease datasets can optimize Random Forest performance through more relevant feature selection [30]. Similar findings were reported in this study where this method produced high F1-score and recall values after the feature selection process [31]. Based on this evidence, the application of RFECV in the classification of premature heart contractions is expected to enhance PAC classification performance, reduce overfitting, and improve inter-patient generalization.

This study proposes a classification framework for premature heart contractions into normal, PAC, and PVC classes by applying RFECV for feature selection and integrating KNN with LightGBM in an ensemble model. This combination aims to produce a model that is both highly accurate and computationally efficient, while also being easy to understand. The study utilizes shapley additive explanations (SHAP) to quantify the contribution of each feature to the decision. This makes the results more transparent and clinically meaningful. This approach should improve the classification of minority classes, such as PAC and PVC, and enhance the model's ability to generalize across patients.

2. METHOD

Figure 1 shows the stages of classifying premature contractions used in this study. These stages include preprocessing, feature extraction, selection of classification features, and evaluation of classification results using parameters recall, precision, and F1-score. All of these stages were systematically designed to ensure the accuracy of ECG signal detection in identifying types of premature contractions.

2.1. Data

The data used in this study are one-dimensional ECG signal data obtained from the MIT-BIH Arrhythmia database [32]. The ECG signals were digitised at a sampling frequency of 360 Hz with 11-bit resolution in the range of 10 mV. There was a total of 48 ECG recordings, each consisting of two channels: the upper MLII channel and the lower V1, V4, V5, and V6 channels, which varied for each recording. In this study, data from only one channel, MLII, were used because the electrical activity recorded by MLII corresponds to the direction of cardiac impulse conduction, and the QRS complex shape is best visualized in the MLII channel [33]. In addition, wearable studies demonstrate that PAC/PVC detection can be performed in a single-lead format (e.g., a 15-second wearable ECG) and that a single lead provides sufficient signal to detect premature beats [34]. In this study, not all ECG recordings were used, only recordings numbered 100, 101, 103, 105, 106, 108, 112, 116, 118, 119, 124, 200, 201, 202, 203, 205, 207, 208, 209, 213, 214, 215, 219, 220, 221, 222, 223, 228, and 232 were used. The determination of these recordings was based on several criteria, including that recording used for training data would not be used for test data and that recordings came from the upper MLII channel (inter-patient). The selection and division of recordings used for training data and test data followed the same selection and division process as those carried out by Shi *et al.* [33].

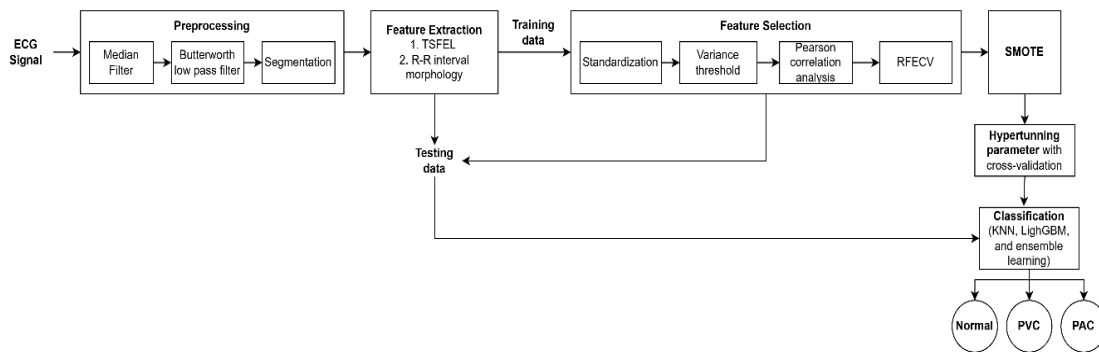


Figure 1. Proposed method

2.2. Preprocessing

The ECG signals obtained from the database were cleaned using a median filter with a width of 200 ms and 600 ms to eliminate baseline wander [26]. Meanwhile, high-frequency power line noise was removed using a Butterworth low-pass filter (LPF) with a cut-off frequency of 40 Hz [26]. Next, PQRST signal segmentation was performed by taking 130 samples before and 170 samples after the R position [35].

2.3. Feature extractions

In this study, various types of features from several domains were used, including temporal, spectral, statistical, and R-R peak interval morphological features. Temporal, spectral, and statistical feature extraction was performed using the time series feature extraction library (TSFEL) available in Python, which provides a variety of features for analysing time signals [36], [37]. Meanwhile, for the R-R interval morphology domain, this study employed four main features: R Position, Pre_R, Post_R, and Local_R [26], [38]. Pre_R is defined as the interval between the observed R and the previous R. Meanwhile, Post_R is the interval between the observed R and the subsequent R, and Local_R is defined as the average of 10 R-R intervals around the observed R.

2.4. Feature selections

Feature selection is performed to reduce computational load. During this stage, feature scaling takes place, followed by the removal of features with low variance. The process continues with Pearson correlation analysis and concludes with feature ranking using RFECV. The features obtained are first scaled to normalise the values, ensuring they fall within the same range. This is done using the standard z-score, which relies on the mean (μ) and standard deviation (s) of the sample. After scaling, features with low variance are removed using the Python library VarianceThreshold(), eliminating those below a set threshold. The remaining features are then checked for correlation; in Python, the Pearson correlation calculates the correlation values. Any features with a correlation above 0.7 are removed, as 0.7 already indicates a very high correlation between two features [39]. Highly correlated features cannot accurately represent the distinct characteristics of the three classes, potentially compromising classification accuracy. Finally, RFECV is employed to rank and select the most predictive features using random forest as an eliminator with 5-fold cross-validation. Starting from all remaining features, RFECV iteratively removes the least important feature based on importance scores obtained from the random forest model trained on the full training set. Each resulting feature subset is evaluated using 5-fold cross-validation, where the same subset is tested across all folds and the validation performance is averaged. The feature subset achieving the highest average cross-validation performance is selected as optimal [40]–[42]. By selecting features based on averaged performance across folds rather than a single data split, RFECV implicitly promotes feature stability, improves generalizability, and reduces the risk of overfitting.

2.5. Classification

In the classification process, the imbalance in the number of annotations between the majority and minority classes in the training data often becomes a serious problem because the model tends to be biased towards the majority class and ignore the minority class. Since the amount of data for the normal, PVC, and PAC classes in the training data is unbalanced, the synthetic minority over-sampling technique (SMOTE) is used as a data balancing method in the training data. SMOTE works by generating synthetic samples in the minority class, not simply duplicating data, but by creating new data through interpolation between existing minority samples and their neighbours in feature space. Thus, the class distribution becomes more balanced, allowing the model to learn patterns from the minority class more effectively, which improves classification performance, particularly on metrics such as recall and F1-score. After data balancing, training and testing are

performed using the selected machine learning models. Hyperparameter tuning for KNN, LightGBM, and the ensemble classifier is conducted using GridSearchCV with stratified 5-fold cross-validation to evaluate combinations of their respective parameters.

2.5.1. KNN

KNN is one of the simplest supervised machine learning algorithms. This means that KNN requires labels as output to recognise patterns between input and output. KNN is a non-parametric algorithm that makes no assumptions about the data. The working principle of KNN is to select a number of K-nearest data points as the basis for determining the class. KNN will calculate the distance from the observed data to all data points in the dataset. Next, the K-nearest data points is selected, and the number of each class is calculated from these K-nearest data points. The data being observed will be classified into the class with the most numerous K-nearest data points around it. Some important parameters in KNN include the number of neighbours ($n_neighbours$) and the weights of each neighbour data point that are taken into consideration. Hyperparameter tuning is performed on both parameters, where the variation in $n_neighbours$ is $n = 4 - 10$. As for the weight, it is “distance” and “uniform”.

2.5.2. LightGBM

LightGBM is an algorithm from the tree-based learning group that utilizes the gradient boosting technique. It works similarly to a decision tree, but the difference lies in how the model builds decision trees iteratively. In LightGBM, each new tree is built to improve on the errors of the previous tree by minimizing the loss function using the gradient descent method. Unlike other algorithms, LightGBM uses a leaf-wise growth approach, whereby trees are developed at leaves that have the greatest potential for loss reduction. This approach makes LightGBM more efficient and capable of producing higher accuracy with fewer iterations, especially on large datasets. To determine the prediction results on new data, LightGBM will sum the contributions of all the trees that have been built. The final result is a combination of all these trees, enabling the model to provide more stable and accurate predictions. To obtain robust results, hyperparameter tuning is performed for several important parameters, including the number of estimators [100, 200], maximum tree depth [3, 5, 7], learning rate [0.001, 0.01, 0.1], maximum number of leaves in each tree [31, 63], and subsample [0.6, 0.8, 1.0].

2.5.3. Ensemble learning

Ensemble learning is a combination of several machine learning algorithms that work together to perform a specific function, such as classification. The advantage of ensemble learning is that it can produce a general and balanced classification method, ensuring that the classification results in each class are not too disparate. The ensemble learning approach employed in this study utilizes a voting classifier strategy with soft voting. Voting classifiers utilise the advantages of each machine learning method used to predict or classify a class. Figure 2 illustrates the operation of the soft voting classifier. In soft voting, each machine learning method does not directly assign a class to the classified data but provides different prediction probabilities (p_n) for each classified class. If there are n classes, each machine learning method will provide p_n for each class. In addition to the prediction probability, another important parameter is the weight (w_j). Machine learning users can determine the weight they want to assign; however, if it is not specified, the system assigns the same weight to each machine learning method. After each machine learning method performs the classification process, the sum of the weight w_j and the prediction probability p_n of each machine learning method will be calculated. The observed data will be classified according to the class with the highest value. Similar to other methods, w_j or the weights for both machine learning models will be varied as follows: [0.9;0.1], [0.8;0.2], [0.7;0.3], [0.6;0.4], [0.5;0.5]. The first number indicates the weight for machine learning 1, and the second number indicates the weight for machine learning 2.

Classification performance is evaluated using precision, recall, and F1-score, which are particularly informative for imbalanced datasets. These metrics are derived from the confusion matrix, which comprises true positives (TP), false positives (FP), true negatives (TN), and false negatives (FN). In addition, McNemar’s test is employed to statistically assess the significance of performance differences between classifiers based on paired predictions on the same test set.

$$Precision = \frac{TP}{TP+FP} \times 100 \quad (1)$$

$$Recall = \frac{TP}{TP+FN} \times 100 \quad (2)$$

$$F1\ score = \frac{2 \times (Precision \times Recall)}{Precision + Recall} \times 100 \quad (3)$$

2.6. SHAP (features interpretation)

SHAP is a method for interpreting machine learning models by fairly measuring the contribution of each feature to a prediction using Shapley values from cooperative game theory [43], [44]. By calculating how predictions change when features are added or removed, SHAP ensures interpretability based on local accuracy, consistency, and the presence of missing values. In this study, SHAP was used to explain the best ensemble model's ECG-based heart contraction classification, providing transparency and clinical relevance.

The SHAP results are visualized in two ways: a summary plot and class-specific plots. In class-specific plots, the x-axis shows the SHAP value, representing the direction and magnitude of each feature's influence on the probability of predicting a given class. Dots represent samples, with color indicating original feature values (red for high, blue for low). Red points on the right indicate that a high feature value increases the likelihood of that class, while blue points on the right or red points on the left show the opposite. The summary plot ranks feature globally by their average absolute SHAP value, highlighting the most influential features in the model.

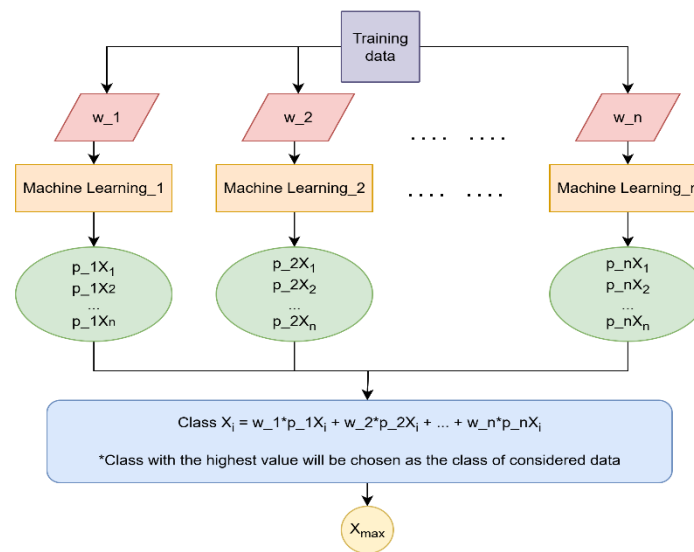


Figure 2. Flow chart soft voting classifier

3. RESULTS AND DISCUSSION

In this section, it is explained the results of research and at the same time is given the comprehensive discussion.

3.1. The classification results of KNN

The selection of hyperparameter $k = 4$ with distance weighting means the KNN model decides based on the four nearest data points. Data closer in distance contributes more to the decision. This makes the model sensitive to the local structure of the data. For example, if there is a 'PAC' class example in an area where most nearby data are 'PVC' or 'N', the model will lean towards the dominant class. Distance weighting reduces the 'vote tie' effect compared to uniform weighting. However, it increases the impact of each nearest data point, which could be an outlier or nearly identical between classes (class overlap). This combination of $k = 4$ and distance weights resulted in high overall accuracy. The trade-off: the minor PAC class suffered from low recall. Although the detection of PAC when predicted was quite accurate, many PAC data points were not recognised as PAC.

Figure 3 show the classification results of KNN. The classification results using KNN showed excellent performance in the normal class, with a recall of 97.45% and a precision of 98.5%, indicating that nearly all normal samples were accurately detected with a very low error rate. In the PVC class, the model was also quite reliable with a recall of 93.39% and precision of 88.47%, although there were still a number of false positives, mainly from the PAC class. Meanwhile, the PAC class had relatively lower performance, as indicated by a recall of 81.1% and a precision of 87.26%, where most of the original PACs were classified as PVC. This indicates feature overlap between PAC and PVC, as well as limitations in the representation of PAC data. Overall, the model's accuracy reached 94.18%, with the primary challenge being to improve the sensitivity of PAC detection.

3.2. The classification results of LightGBM

After the tuning process, the LightGBM model was selected with the following parameters: $n_estimators = 200$, $learning_rate = 0.1$, $max_depth = 5$, $num_leaves = 31$, and partial sample and feature settings, specifically $subsample = 0.8$. This combination balances model complexity and generalisation ability: $max_depth = 5$ limits the maximum depth of the tree so that it is not too deep, thereby reducing the risk of overfitting; $num_leaves = 31$ provides an adequate number of leaves so that the tree is still flexible enough to capture data variations in each boosting iteration, but is not too complicated. $Learning_rate = 0.1$ sets a moderate learning speed, allowing many trees (ensembles) to contribute gradually, while $n_estimators = 200$ provides enough boosting rounds for the model to learn complex patterns. The $subsample$ setting of 0.8 (selecting 80% of data rows per iteration) introduces an element of randomness that helps reduce overfitting and improve robustness. The random state is set so that the results can be reproduced. Overall, this tuning appears to have successfully created a good trade-off between bias and variance, enabling the model to generalize strongly while still capturing important patterns without excessive overfitting.

In this study Figure 4 show the classification results of LightGBM, the classification model demonstrated a very high capability in recognizing class N, with a precision of around 98.15% and a recall of nearly 99.82%, resulting in a class N F1-score of approximately 98.98%. This means that the model made almost no mistakes in predicting samples from class N, where out of 2,237 data points, only 4 were misclassified. For the PVC class, the performance was also quite good: PVC recall was around 95.38%, while precision was in the range of 88.22%, resulting in an F1-score of 91.66%. This indicates that most PVC samples were successfully recognized, although there were still prediction errors from other classes, especially PAC, which was also misclassified as PVC. The PAC class, despite achieving a high precision of 95.19%, experienced a significant decrease in recall of approximately 71.49%, resulting in a PAC F1-score of only 81.65%. This reflects that although many data were successfully classified as PAC, 27% of PAC samples were not identified as PAC and were classified into the PVC class. The difference in metrics between classes clearly shows that the model's performance is more consistent and reliable for classes with higher prevalence, such as N and PVC. In contrast, for minority classes, such as PAC, despite high precision, sensitivity remains relatively low in this dataset and evaluation setting.

3.3. The classification results of ensemble learning

In this ensemble learning approach, KNN and LightGBM were utilized with parameters derived from previous hyperparameter tuning. Meanwhile, the soft voting weights that yielded the optimum results were [0.6, 0.4] for each machine learning model. The classification results in Figure 5 obtained indicate that the model exhibits very high performance for the N class, with a precision of approximately 98.75% and a recall of approximately 99.06%, resulting in an F1-score of approximately 98.90%. These figures indicate that the model almost always succeeds in correctly recognising N samples and makes very few false positives and false negatives in this class. For the PVC class, the performance is also strong. The precision of PVC predictions reaches 90.59%, indicating that most PVC predictions are correct, although there are a number of incorrect predictions from other classes. The PVC recall reaches 94.43%, meaning that most PVC samples are successfully identified. The F1-score for the PVC class reached 92.47%, indicating a good balance between precision and recall for the PVC class, although not as high as that of the N class. Meanwhile, the PAC class showed slightly different results. The PAC precision was quite high, reaching 89.91%, indicating that when the model predicted PAC, the prediction was relatively reliable. However, the PAC recall is lower, at around 80.52%, which means that a proportion of PAC data is not successfully detected as PAC (approximately 19-20% of PAC samples are predicted as other classes, especially PVC). The PAC F1-score is approximately 84.96%, indicating that although the PAC prediction is quite precise, the overall performance of the PAC class is still affected by the relatively low recall value. The differences in these metrics consistently show that classes with higher prevalence (particularly the N class) achieve the most optimal performance, while minority classes, such as PAC, despite obtaining good precision, still experience a gap in sensitivity (recall). In the context of applications where errors in detecting the PAC class carry significant weight, the lower recall of PAC becomes a critical point in interpreting performance. For scientific reports, the margin between precision and recall for each class is important to note, as it indicates the model's bias towards the dominant class in the dataset, and shows that an overall evaluation using only accuracy or global metrics may mask the relatively weak performance on smaller classes [45]. In this study, soft voting weights were varied using discrete increments to provide a transparent and computationally efficient comparison. While this approach was sufficient for identifying an effective ensemble configuration, more advanced optimization methods such as Bayesian optimization or evolutionary algorithms could be explored in future work to potentially further improve ensemble performance.

True Label	N	2180	48	9
	PVC	20	990	50
	PAC	13	81	404
		N	PVC	PAC
		Predicted Label		

Figure 3. Confusion matrix of KNN

True Label	N	2233	3	1
	PVC	32	1011	17
	PAC	10	132	356
		N	PVC	PAC
		Predicted Label		

Figure 4. Confusion matrix of LightGBM

True Label	N	2216	16	5
	PVC	19	1001	40
	PAC	9	88	401
		N	PVC	PAC
		Predicted Label		

Figure 5. Confusion matrix of ensemble learning

3.4. Discussion

Table 1 shows the classification results of the KNN, LightGBM, and ensemble learning algorithms. In evaluating performance between single methods and ensemble methods, LightGBM showed sufficient performance and prediction stability compared to KNN. LightGBM, a tree-based gradient boosting algorithm, captures complex feature interactions through a leaf-wise growth strategy that iteratively selects the leaf with the maximum loss reduction, often leading to deeper trees and better predictive performance [46], [47]. Conversely, KNN has an advantage in recall or sensitivity in classifying PAC. This is because KNN is a method that relies on the nearest neighbouring class in the feature space, so when PAC samples are in a local cluster that has similar, KNN will be better able to classify the PAC class correctly, even though the number of PACs is smaller than other classes. Meanwhile, LightGBM is very effective in global error optimisation, making it less responsive to rare local patterns (which appear in minor classes), particularly when such patterns contribute minimally to overall loss reduction during boosting.

On the other hand, the KNN–LightGBM ensemble successfully combines the advantages of both methods and utilises LightGBM’s strength in handling non-linear features and dataset complexity, as well as KNN’s ability to provide sensitivity to local variability, so that this ensemble shows an improvement in metrics such as recall and F1-score in minor classes compared to the two single methods. More generally, ensemble approaches tend to achieve better results in imbalanced data [48]–[51]. This trend is reflected in our findings, where the ensemble model shows enhanced detection performance especially for minority classes such as PVC and PAC. Therefore, from a scientific point of view, the KNN–LightGBM ensemble method was chosen as the preferred method because the research objective emphasised the best performance in the PVC and PAC classes. To substantiate the observed performance differences, McNemar’s test was applied to paired predictions generated from the same test set. The results indicate that the ensemble model significantly outperforms KNN ($p = 7.66 \times 10^{-8}$), while no statistically significant difference is observed between the ensemble model and LightGBM ($p = 0.1359$), suggesting comparable predictive performance. Importantly, the absence of statistical significance relative to LightGBM indicates performance equivalence rather than inferiority. Therefore, the ensemble approach remains preferable due to its higher F1-score for the PVC and PAC classes, which are central to the objectives of this study, as well as its increased robustness achieved through the integration of heterogeneous classifiers [52].

Based on the comparison results in Table 2, this study shows better performance compared to most previous studies, especially in terms of the average F1-score, which reached 88.72%, higher than Mateo and Talavera (71.42%) [23], Yang *et al.* (82.40%) [27], Gusev (85.01%) [24], Zakaria *et al.* (84.92%) [26], and Deng *et al.* (average not recorded) [25]. For the PVC class, this study recorded a precision of 90.59%, a recall of 94.43%, and an F1-score of 92.47%. These values are relatively balanced between precision and recall, and are superior to Zakaria *et al.* (76%) [26] and Deng *et al.* (72.96%) [25]. In fact, its performance is comparable to that of Mateo and Talavera (92.30%) [23] and Yang *et al.* (92.60%) [27], but with an advantage in the balance between precision and recall. This demonstrates that the method employed is capable of reducing PVC classification errors without compromising sensitivity. For the PAC class, this study produced a precision of 89.91%, a recall of 80.52%, and an F1-score of 84.96%. Compared to Mateo *et al.*, who achieved an F1-score of only 50.58%, the improvement is very significant. However, when compared to Zakaria *et al.* (F1-score of 93.83%) [26] or Deng *et al.* (recall of 89.45%) [25], this study still lags slightly in sensitivity, especially in recognising PAC, which is relatively fewer in number. Nevertheless, the precision of PAC in this study is much higher than in most other studies, indicating a lower prediction error rate when the model classifies PAC. In addition, the classification of PVC and PAC in this study generally yields good and relatively balanced results, compared to other studies that often show significant differences in performance between PVC and PAC.

These results indicate that the feature selection process effectively reduced the dimensionality of the feature space, enabling the model to learn more efficiently while focusing on the most informative variables. Initially, Pearson correlation filtering was applied with a threshold of 0.7 to remove strongly redundant features, simplifying the feature set before the main selection process. Subsequently, RFECV was performed, using cross-validation at each iteration to systematically evaluate feature importance and retain only those that contributed significantly to classification performance. This staged elimination approach not only prevented overfitting caused by an excessive number of features but also improved model generalization and produced a simpler yet meaningful representation of the data for clinical analysis [53]. RFECV selected several important features, grouped as follows: morphological features (Pre_R, Local_R, Post_R); statistical features such as median and kurtosis; spectral features such as median frequency, spectral distance, and spectral. While the Pearson correlation threshold of 0.7 proved effective, alternative thresholds or other multicollinearity diagnostics could be explored in future work to further refine feature quality.

Table 1. The classification results of all algorithms

	Class	Precision	Recall	F1-Score	Accuracy
KNN	N	98.50%	97.45%	97.97%	94.18%
	PVC	88.47%	93.39%	90.86%	
	PAC	87.26%	81.12%	84.08%	
LightGBM	N	98.15%	99.82%	98.98%	94.86%
	PVC	88.22%	95.38%	91.66%	
	PAC	95.19%	71.49%	81.65%	
Ensemble learning	N	98.75%	99.06%	98.90%	95.34%
	PVC	90.59%	94.43%	92.47%	
	PAC	89.91%	80.52%	84.96%	

Table 2. Comparison with other research

Other research	PVC			PAC			Average of
	Precision	Recall	F1-score	Precision	Recall	F1-score	F1-score
Mateo and Talavera [23]	89.40%	95.38%	92.30%	51.95%	49.26%	50.58%	71.42%
Yang <i>et al.</i> [27]			92.60%			72.20%	82.40%
Gusev [24]							85.01%
Zakaria <i>et al.</i> [26]	76%	76%	76%	90%	98%	93.83%	84.92%
Deng <i>et al.</i> [25]		72.96%			89.45%		
This study	90.59%	94.43%	92.47%	89.91%	80.52%	84.96%	88.72%

3.5. SHAP-features interpretation

The results of interpreting the VotingClassifier (KNN+LightGBM) model using SHAP KernelExplainer show that the R interval, spectral, and statistical features play a crucial role in distinguishing between the normal, PAC, and PVC classes. The main influential features are Pre_R, Median frequency, Spectral distance, Local_R, median, and kurtosis. The SHAP Kernel method offers high flexibility in explaining ensemble models; however, the results can be unstable due to its reliance on stochastic sampling, which may yield different attributions across runs. Recent studies have shown that Kernel SHAP's instability stems from its random neighbor selection procedure [54]. In future work, repeated SHAP analyses or corroboration using alternative explainability methods such as LIME and permutation feature importance could be employed to further assess the robustness of feature attributions [55], [56].

Figures 6 to 8 show the list of top features for each class. In the normal class, high Pre_R values almost always increase the probability of a normal prediction. This effect is reinforced by statistical features such as median and kurtosis the higher these values, the greater the support for normal classification. In the PAC class, Pre_R, Median frequency, and Spectral distance play a major role. Low values of Pre_R, Median frequency, Spectral distance, and Local_R generally increase the PAC prediction, as shown by blue dots on the right side (positive SHAP values). The red dots on the right also indicate that, under certain conditions, high values of these features can still increase the probability of PAC, suggesting feature interactions. Thus, PAC can be triggered by low-value features or from a combination of high feature values with other factors. In the PVC class, a similar pattern occurs: Pre_R remains dominant; Spectral distance and Median frequency follow as key features in detecting premature ventricular beats. The blue and red dots for Pre_R on the right side indicate that both high and low values can increase PVC prediction, depending on the context of other features. For Spectral distance and Median frequency, high values consistently increase PVC probability. For Absolute energy, low values drive the prediction toward the PVC class.

Figure 9 shows the list of top features based on SHAP values. The top five features Pre_R, Median frequency, Spectral distance, Local_R, and Absolute energy were selected by the model. They are physiologically linked to premature beats (both PAC and PVC) and normal rhythm. Pre_R represents the interval or characteristics before the R wave. Premature beats typically affect the R-to-R interval or the waveform around R, making features that measure the interval before or after R highly informative [34]. The Median frequency and Spectral distance features describe changes in frequency content when the signal shows abnormal fluctuations, such as premature beats, noise, or R-R interval variations. Local_R likely captures local changes in the signal around the R wave. These include abnormal R-R interval changes or unusual shapes before or after R, which signal premature beats. The Absolute energy feature reflects the total ‘strength’ of the signal. Premature beats often cause energy surges or amplitude fluctuations, thereby increasing the overall signal energy relative to normal signals [57], [58].

Importantly, these feature-level insights can assist clinicians by highlighting which signal characteristics are most informative for distinguishing premature beats, potentially supporting more focused ECG interpretation and monitoring strategies. From a system development perspective, the identification of these key features may also guide future data collection and model refinement by prioritizing physiologically relevant signal characteristics. Nevertheless, the identified features originate from the specific model and dataset used in this study and do not constitute clinical confirmation. Broader clinical data, inter-patient evaluation, and external validation are required before these insights can be reliably applied in medical practice.

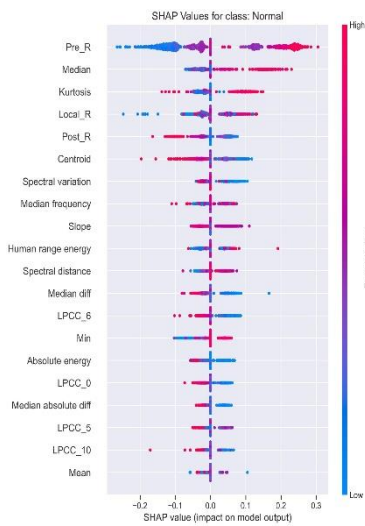


Figure 6. SHAP for normal

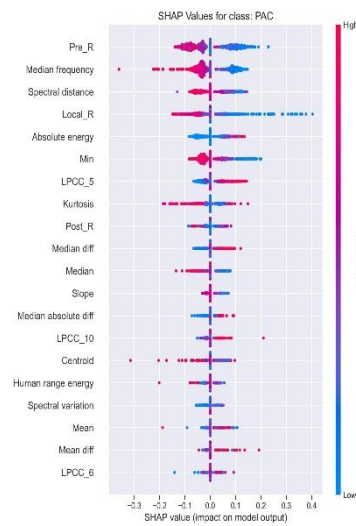


Figure 7. SHAP for PAC

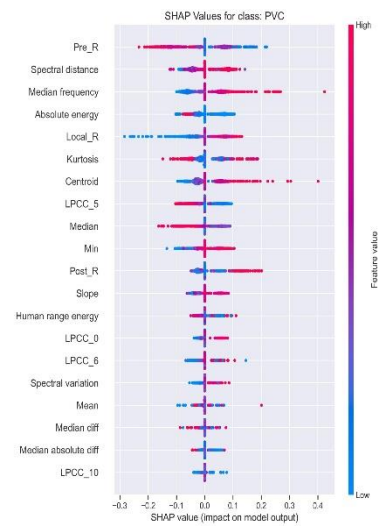


Figure 8. SHAP for PVC

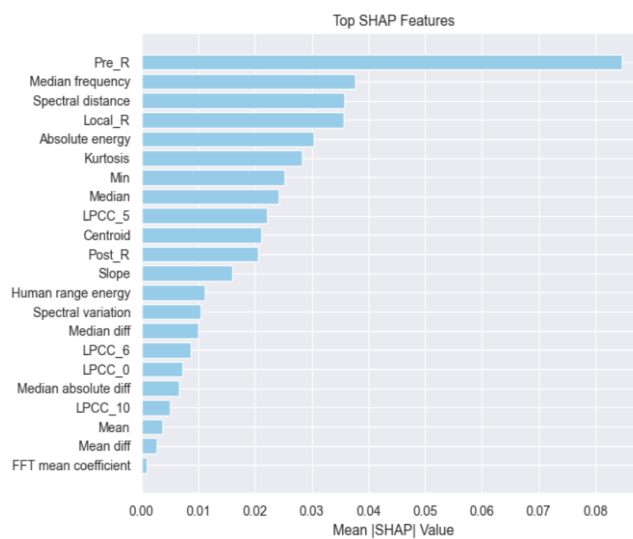


Figure 9. SHAP summary plot-top features

4. CONCLUSION

This study proposes a robust framework for classifying premature cardiac contractions using RFECV-based feature selection and an ensemble of KNN and LightGBM. The model achieves high and balanced performance across normal, PVC, and PAC classes, including under inter-patient validation, demonstrating its reliability and competitiveness with existing approaches. SHAP-based interpretability analysis confirms that features such as Pre_R, median frequency, spectral distance, Local_R, and absolute energy are the most informative, supporting physiological relevance and clinical interpretability. Beyond performance improvements, this framework provides a foundation for developing reliable and explainable arrhythmia detection systems that can support wearable monitoring and clinical decision-support applications. Future work will focus on validation using larger and more diverse patient populations, integration with deep learning approaches, and evaluation of real-time implementation for practical clinical deployment.

ACKNOWLEDGMENTS

This research was supported by LPPM Universitas Jenderal Soedirman through UNSOED BLU Research Grant 2025.

FUNDING INFORMATION

The authors would like to thank LPPM Universitas Jenderal Soedirman for funding this research through the UNSOED BLU Research Grant 2025.

AUTHOR CONTRIBUTIONS STATEMENT

This journal uses the Contributor Roles Taxonomy (CRediT) to recognize individual author contributions, reduce authorship disputes, and facilitate collaboration.

Name of Author	C	M	So	Va	Fo	I	R	D	O	E	Vi	Su	P	Fu
Elsa Sari Hayunah Nurdiniyah	✓	✓	✓	✓	✓	✓	✓	✓	✓	✓			✓	✓
A'isyah Nur Aulia Yusuf		✓		✓	✓			✓	✓	✓	✓	✓	✓	✓
Norma Amalia					✓		✓			✓	✓	✓		✓
Widhiatmoko Herry Purnomo						✓				✓	✓	✓		✓
Azizah Najda Hafizha						✓			✓		✓		✓	

- C : **C**onceptualization
- M : **M**ethodology
- So : **S**oftware
- Va : **V**alidation
- Fo : **F**ormal analysis
- I : **I**nvestigation
- R : **R**esources
- D : **D**ata Curation
- O : **O**riginal Draft
- E : **E**diting
- Vi : **V**isualization
- Su : **S**upervision
- P : **P**roject administration
- Fu : **F**unding acquisition

CONFLICT OF INTEREST STATEMENT

There is no conflict of interest in this research.

INFORMED CONSENT

We have obtained informed consent from all individuals included in this study.

ETHICAL APPROVAL

The study utilized open access database (<https://physionet.org/content/mitdb/1.0.0/>) and therefore did not require ethical approval, as it complied with all relevant national regulations and institutional policies.

DATA AVAILABILITY

The data that support the findings of this study are openly available in <https://physionet.org/content/mitdb/1.0.0/> at <https://doi.org/10.13026/C2F305>.




REFERENCES

- [1] H. Yang and Z. Wei, "A novel approach for heart ventricular and atrial abnormalities detection via an ensemble classification algorithm based on ECG morphological features," *IEEE Access*, vol. 9, pp. 54757–54774, 2021, doi: 10.1109/access.2021.3071273.
- [2] J. C. L. Himmelreich *et al.*, "Frequent premature atrial contractions are associated with atrial fibrillation, brain ischaemia, and mortality: a systematic review and meta-analysis," *EP Europace*, vol. 21, no. 5, pp. 698–707, Dec. 2018, doi: 10.1093/europace/euy276.
- [3] Y. Shimada *et al.*, "Higher frequency of premature atrial contractions correlates with atrial fibrillation detection after cryptogenic stroke," *Stroke*, vol. 55, no. 4, pp. 946–953, Apr. 2024, doi: 10.1161/STROKEAHA.123.044813.
- [4] J. M. Farinha, D. Gupta, and G. Y. H. Lip, "Frequent premature atrial contractions as a signalling marker of atrial cardiomyopathy, incident atrial fibrillation, and stroke," *Cardiovascular Research*, vol. 119, no. 2, pp. 429–439, Apr. 2022, doi: 10.1093/cvr/cvac054.
- [5] C.-Y. Chen *et al.*, "High premature atrial complex burden and risk of renal function decline," *Clinical Kidney Journal*, vol. 17, no. 8, 2024, doi: 10.1093/ckj/sfae208.
- [6] D. Han *et al.*, "Premature atrial and ventricular contraction detection using photoplethysmographic data from a smartwatch," *Sensors*, vol. 20, no. 19, p. 5683, Oct. 2020, doi: 10.3390/s20195683.
- [7] Y. G. Kim *et al.*, "Premature ventricular contraction increases the risk of heart failure and ventricular tachyarrhythmia," *Scientific Reports*, vol. 11, no. 1, 2021, doi: 10.1038/s41598-021-92088-0.
- [8] P. Lee, M. Huang, T. Huang, C. Hsu, S. Lin, and P. Liu, "High burden of premature ventricular complex increases the risk of new-onset atrial fibrillation," *Journal of the American Heart Association*, vol. 12, no. 4, Feb. 2023, doi: 10.1161/JAHA.122.027674.
- [9] F. De Marco, F. Ferrucci, M. Risi, and G. Tortora, "Classification of QRS complexes to detect premature ventricular contraction using machine learning techniques," *PLOS ONE*, vol. 17, no. 8, p. e0268555, Aug. 2022, doi: 10.1371/journal.pone.0268555.
- [10] M. H. Mazidi, M. Eshghi, and M. R. Raoufy, "Detection of premature ventricular contraction (PVC) using linear and nonlinear techniques: an experimental study," *Cluster Computing*, vol. 23, no. 2, pp. 759–774, Jun. 2020, doi: 10.1007/s10586-019-02953-x.
- [11] R. M. Devadas, "Cardiac arrhythmia classification using SVM, KNN and naive Bayes algorithms," *International Research Journal of Engineering and Technology (IRJET)*, vol. 08, no. 05, pp. 3937–3941, 2021.
- [12] M. Jannah and A. A. Nababan, "Optimization of KNN classification for ECG data analysis: comparative study of model performance using the hyperparameter tuning and cross-validation," *International Journal of Electronics and Communications Systems*, vol. 5, no. 1, pp. 105–116, Jun. 2025, doi: 10.24042/ijecs.v5i1.28467.
- [13] S. Manao, D. Sitanggang, A. Sagala, A. Oktarino, and M. Turnip, "Application of KNN method for classification of arrhythmia types based on ECG data," *Journal of Computer Networks, Architecture and High Performance Computing*, vol. 7, no. 3, pp. 629–637, Jul. 2025, doi: 10.47709/cnahpc.v7i3.6010.
- [14] M. S. Vural, K. Heryan, S. Sיעיński, P. Bilko, and M. Grzegorzec, "Classification of the Heartbeats in Electrocardiograms with K-Nearest Neighbors Algorithm, Random Forests, and Support Vector Machines - A Pilot Study," *Lecture Notes in Networks and Systems. Springer Nature Switzerland*, pp. 177–184, 2025. doi: 10.1007/978-3-031-82143-1_20.
- [15] Z. C. Oleiwi, E. N. AlShemmary, and S. Al-Augby, "Arrhythmia detection based on new multi-model technique for ECG inter-patient classification," *International Journal of Online and Biomedical Engineering (iJOE)*, vol. 19, no. 12, pp. 78–98, Aug. 2023, doi: 10.3991/ijoe.v19i12.41631.
- [16] C. U. Kumari, A. S. D. Murthy, B. L. Prasanna, M. P. P. Reddy, and A. K. Panigrahy, "An automated detection of heart arrhythmias using machine learning technique: SVM," *Materials Today: Proceedings*, vol. 45, pp. 1393–1398, 2021, doi: 10.1016/j.matpr.2020.07.088.
- [17] Z. Liu, Z. Tian, Y. Zhou, H. Li, and B. Dong, "Analysis of arrhythmia features based on LightGBM and kmeans feature extraction," *Highlights in Science, Engineering and Technology*, vol. 56, pp. 271–279, 2023, doi: 10.54097/hset.v56i.10583.
- [18] T. N. Vo, "Heart rate classification in ECG signals using machine learning and deep learning," *arXiv*, Jun. 2025, doi: 10.48550/arXiv.2506.06349.
- [19] S. Bhattacharyya, S. Majumder, P. Debnath, and M. Chanda, "Arrhythmic heartbeat classification using ensemble of random forest and support vector machine algorithm," *IEEE Transactions on Artificial Intelligence*, vol. 2, no. 3, pp. 260–268, Jun. 2021, doi: 10.1109/TAI.2021.3083689.
- [20] M. Sraith, Y. Jabrane, and A. Atlas, "An overview on intra- and inter-patient paradigm for ECG heartbeat arrhythmia classification," in *2021 International Conference on Digital Age & Technological Advances for Sustainable Development (ICDATA)*, IEEE, Jun. 2021, pp. 1–7. doi: 10.1109/ICDATA52997.2021.00011.
- [21] P. Yang, D. Wang, W.-B. Zhao, L.-H. Fu, J.-L. Du, and H. Su, "Ensemble of kernel extreme learning machine based random forest classifiers for automatic heartbeat classification," *Biomedical Signal Processing and Control*, vol. 63, p. 102138, Jan. 2021, doi: 10.1016/j.bspc.2020.102138.
- [22] S. Mandala *et al.*, "An improved method to detect arrhythmia using ensemble learning-based model in multi lead electrocardiogram (ECG)," *PLOS ONE*, vol. 19, no. 4, p. e0297551, Apr. 2024, doi: 10.1371/journal.pone.0297551.
- [23] C. Mateo and J. A. Talavera, "Analysis of atrial and ventricular premature contractions using the short time Fourier transform with the window size fixed in the frequency domain," *Biomedical Signal Processing and Control*, vol. 69, p. 102835, Aug. 2021, doi: 10.1016/j.bspc.2021.102835.
- [24] M. Gusev, "Detection of premature heartbeats," in *2022 45th Jubilee International Convention on Information, Communication and Electronic Technology (MIPRO)*, IEEE, May 2022, pp. 350–355. doi: 10.23919/mipro55190.2022.9803747.
- [25] J. Deng, H. Yang, and Y. Liu, "ECG signal classification based on sparse representation and SVM," *IET Conference Proceedings*, vol. 2023, no. 30, pp. 5–8, Dec. 2023, doi: 10.1049/icp.2023.3276.
- [26] H. Zakaria, E. S. H. Nurdiniyah, A. M. Kurniawati, D. Naufal, and N. Sutisna, "Morphological arrhythmia classification based on inter-patient and two leads ECG using machine learning," *IEEE Access*, vol. 12, pp. 147372–147386, 2024, doi: 10.1109/access.2024.3469640.
- [27] J. Yang, W. Cai, and M. Wang, "Premature beats detection based on a novel convolutional neural network," *Physiological Measurement*, vol. 42, no. 7, p. 75003, 2021, doi: 10.1088/1361-6579/ac0e82.
- [28] A. Odugoudar and J. S. Walia, "ECG classification system for arrhythmia detection using convolutional neural networks," *arXiv*, Jun. 2024, doi: 10.48550/arXiv.2303.03660.




- [29] J. Zhu, H. Liu, X. Liu, C. Chen, and M. Shu, "Cardiovascular disease detection based on deep learning and multi-modal data fusion," *Biomedical Signal Processing and Control*, vol. 99, p. 106882, Jan. 2025, doi: 10.1016/j.bspc.2024.106882.
- [30] T. A. Assegie, P. K. Rangarajan, N. K. Kumar, and D. Vigneswari, "An empirical study on machine learning algorithms for heart disease prediction," *IAES International Journal of Artificial Intelligence (IJ-AI)*, vol. 11, no. 3, p. 1066, 2022, doi: 10.11591/ijai.v11.i3.pp1066-1073.
- [31] S. P. Aulia, B. Rahmat, and A. Junaidi, "Enhancing heart disease prediction through SMOTE-ENN balancing and RFECV feature selection," *Journal of Artificial Intelligence and Engineering Applications (JAIEA)*, vol. 4, no. 3, pp. 1968–1973, 2025, doi: 10.59934/jaiea.v4i3.1057.
- [32] A. L. Goldberger *et al.*, "PhysioBank, PhysioToolkit, and PhysioNet: components of a new research resource for complex physiologic signals," *Circulation*, vol. 101, no. 23, 2000, doi: 10.1161/01.cir.101.23.e215.
- [33] H. Shi, H. Wang, F. Zhang, Y. Huang, L. Zhao, and C. Liu, "Inter-patient heartbeat classification based on region feature extraction and ensemble classifier," *Biomedical Signal Processing and Control*, vol. 51, pp. 97–105, May 2019, doi: 10.1016/j.bspc.2019.02.012.
- [34] M. Orini *et al.*, "Premature atrial and ventricular contractions detected on wearable-format electrocardiograms and prediction of cardiovascular events," *European Heart Journal - Digital Health*, vol. 4, no. 2, pp. 112–118, Feb. 2023, doi: 10.1093/ehjdh/zta007.
- [35] J. Jiang, H. Zhang, D. Pi, and C. Dai, "A novel multi-module neural network system for imbalanced heartbeats classification," *Expert Systems with Applications: X*, vol. 1, p. 100003, Apr. 2019, doi: 10.1016/j.eswax.2019.100003.
- [36] M. Barandas *et al.*, "TSFEL: time series feature extraction library," *SoftwareX*, vol. 11, p. 100456, Jan. 2020, doi: 10.1016/j.softx.2020.100456.
- [37] I. H. Tsai and B. I. Morshed, "Signal-specific and signal-independent features for real-time beat-by-beat ECG classification with AI for cardiac abnormality detection," *Electronics*, vol. 14, no. 13, p. 2509, 2025, doi: 10.3390/electronics14132509.
- [38] A. Srinivasulu and N. Sriraam, "Signal processing framework for the detection of ventricular ectopic beat episodes," *Journal of Medical Signals & Sensors*, vol. 13, no. 3, pp. 239–251, 2023, doi: 10.4103/jmss.jmss_12_22.
- [39] M. M. Mukaka, "Statistics corner: a guide to appropriate use of correlation coefficient in medical research," *Malawi Medical Journal*, vol. 24, no. 3, pp. 69–71, 2012.
- [40] "RFECV — scikit-learn 1.8.0 documentation," Scikit-Learn. Accessed: Jan. 16, 2026. [Online]. Available: https://sklearn.org/1.8/modules/generated/sklearn.feature_selection.RFECV
- [41] M. Awad and S. Fraihat, "Recursive feature elimination with cross-validation with decision tree: feature selection method for machine learning-based intrusion detection systems," *Journal of Sensor and Actuator Networks*, vol. 12, no. 5, p. 67, 2023, doi: 10.3390/jsan12050067.
- [42] T.-H. Sun, C.-C. Wang, Y.-L. Wu, K.-C. Hsu, and T.-H. Lee, "Machine learning approaches for biomarker discovery to predict large-artery atherosclerosis," *Scientific Reports*, vol. 13, no. 1, 2023, doi: 10.1038/s41598-023-42338-0.
- [43] S. M. Lundberg and S.-I. Lee, "A unified approach to interpreting model predictions," in *31st Conference on Neural Information Processing Systems (NIPS 2017)*, Long Beach, CA, USA., 2017, pp. 1–10.
- [44] S. M. Lundberg *et al.*, "Explainable machine-learning predictions for the prevention of hypoxaemia during surgery," *Nature Biomedical Engineering*, vol. 2, no. 10, pp. 749–760, Oct. 2018, doi: 10.1038/s41551-018-0304-0.
- [45] K. M. Sujon, R. Hassan, K. Choi, and M. A. Samad, "Accuracy, precision, recall, f1-score, or MCC? empirical evidence from advanced statistics, ML, and XAI for evaluating business predictive models," *Journal of Big Data*, vol. 12, no. 1, Dec. 2025, doi: 10.1186/s40537-025-01313-4.
- [46] K. Taha, "Tree-based ensemble learning models for protein-protein interactions detection: a review and experimental evaluation," *BioData Mining*, vol. 19, no. 1, Nov. 2025, doi: 10.1186/s13040-025-00501-5.
- [47] H. Talebi, A. K. Bardsiri, and V. K. Bardsiri, "Developing a hybrid machine learning model for employee turnover prediction: Integrating LightGBM and genetic algorithms," *Journal of Open Innovation: Technology, Market, and Complexity*, vol. 11, no. 2, p. 100557, 2025, doi: 10.1016/j.joitmc.2025.100557.
- [48] M. A. Mim, N. Majadi, and P. Mazumder, "A soft voting ensemble learning approach for credit card fraud detection," *Heliyon*, vol. 10, no. 3, p. e25466, Feb. 2024, doi: 10.1016/j.heliyon.2024.e25466.
- [49] N. El Furqany, "Hybrid ensemble learning with SMOTEENN and soft voting for stunting risk prediction: A SHAP-based explainable approach," *Journal of Applied Data Sciences*, vol. 6, no. 4, pp. 2989–3004, 2025, doi: 10.47738/jads.v6i4.829.
- [50] J. Unjung *et al.*, "Soft voting ensemble model to improve Parkinson's disease prediction with SMOTE," *International Journal of Advances in Intelligent Informatics*, vol. 11, no. 1, p. 120, Feb. 2025, doi: 10.26555/ijain.v11i1.1627.
- [51] J. F. Hammadi, A. B. A. Latif, and Z. B. C. Cob, "An Improved Framework for Cardiovascular Disease Prediction using Hybrid Ensemble Learning Soft-Voting Model," *International Journal of Computational and Experimental Science and Engineering (IJCESEN)*, vol. 11, no. 3, Jun. 2025, doi: 10.22399/ijcesen.2348.
- [52] Á. Kovács, R. Gunics, G. Kovásznai, and T. Tajti, "Soft voting robustness in neural network ensembles with empirical analysis and formal verification," *Annales Mathematicae et Informaticae*, vol. 61, pp. 171–185, 2025, doi: 10.33039/ami.2025.10.002.
- [53] J. Sung *et al.*, "Classification of stroke severity using clinically relevant symmetric gait features based on recursive feature elimination with cross-validation," *IEEE Access*, vol. 10, pp. 119437–119447, 2022, doi: 10.1109/ACCESS.2022.3218118.
- [54] G. Kelodjou *et al.*, "Shaping up SHAP: enhancing stability through layer-wise neighbor selection," *Proceedings of the AAAI Conference on Artificial Intelligence*, vol. 38, no. 12, pp. 13094–13103, Mar. 2024, doi: 10.1609/aaai.v38i12.29208.
- [55] N. Nabuoso, "Evaluating LIME and SHAP in explaining malnutrition classification in children under five," in *Proceedings of the 14th International Conference on Pattern Recognition Applications and Methods*, SCITEPRESS - Science and Technology Publications, 2025, pp. 291–298. doi: 10.5220/0013186500003905.
- [56] L. Lin and Y. Wang, "SHAP stability in credit risk management: a case study in credit card default model," *Risks*, vol. 13, no. 12, p. 238, Dec. 2025, doi: 10.3390/risks13120238.
- [57] G. D. Clifford, *ECG statistics, noise, artifacts, and missing data*. Massachusetts Institute of Technology, 2006.
- [58] V. Sharmila and K. A. Reddy, "Identification of premature ventricular cycles of electrocardiogram using discrete cosine transform-Teager energy operator model," *Journal of Medical Engineering*, vol. 2015, pp. 1–9, Mar. 2015, doi: 10.1155/2015/438569.

BIOGRAPHIES OF AUTHORS






Elsa Sari Hayunah Nurdiniyah    received her Bachelor degree in Engineering Physics, from Universitas Gadjah Mada, Indonesia, in 2018 and Master degree in Electrical Engineering from School of Electrical Engineering and Informatics, Institut Teknologi Bandung, in 2022. She is currently a lecturer in Department of Electrical Engineering, University Jenderal Soedirman. Her research interests are in the areas of signal processing, biomedical signals, machine learning and data analysis. She can be contacted at email: elsa.nurdiniyah@unsoed.ac.id.






A'isyah Nur Aulia Yusuf    received the Bachelor of Engineering degree in Information Technology from the Universitas Gadjah Mada, Yogyakarta, Indonesia, in 2018, and the Master's degree in Electrical Engineering from the University of Indonesia, Depok, Indonesia, in 2021. She is a PMDSU scholarship awardee and a Doctor candidate at the University of Indonesia. She is currently a lecturer in Department of Electrical Engineering, Universitas Jenderal Soedirman. Her research interest is machine learning, antenna, telecommunication, and IoT. She can be contacted at email: aisyah.yusuf@unsoed.ac.id.






Norma Amalia    is a lecturer and researcher at Universitas Jenderal Soedirman, Indonesia. She earned her Bachelor's degree in Telecommunication Engineering from Telkom University and her Master's degree in Electrical Engineering from Universitas Gadjah Mada. Her research focuses on telecommunications and communication systems, with particular interests in signal processing, wireless networks, and emerging technologies that enhance connectivity and digital literacy. She can be contacted at email: norma.amalia@unsoed.ac.id.



Widhiatmoko Herry Purnomo    received the B.Eng. degree in Electrical Engineering from Universitas Gadjah Mada (UGM), Indonesia, and the M.Eng. degree from Institut Teknologi Bandung (ITB), Bandung, Indonesia. He is a lecturer and researcher at the Department of Electrical Engineering, Faculty of Engineering, Universitas Jenderal Soedirman (UNSOED), Indonesia, with expertise in telecommunications, wireless communication systems, and signal processing. His research interests encompass telecommunications, wireless communication systems, and signal processing, with a particular emphasis on the advancement of contemporary communication technologies and their practical applications. His scholarly work further extends to areas such as optical communication networks, quality of service (QoS) for multimedia transmission, channel modeling and propagation analysis, as well as the development of efficient communication and power systems for rural applications, including pico-hydro technology. In addition, he has been actively involved in academic development and community engagement, particularly through initiatives in education, research, and collaborative programs that strengthen the linkage between the university and society. He can be contacted at email: widhiatmoko.purnomo@unsoed.ac.id.



Azizah Najda Hafizha    is an undergraduate student in the Department of Electrical Engineering at Jenderal Soedirman University. She has a profound interest and focuses in the field of computer and information engineering. Her specific interests include software engineering, artificial intelligent, and machine learning. She can be contacted at email: azizah.hafizha@mhs.unsoed.ac.id.